Interaction of a planar shock with a blast wave

Jiming Yang[2], Mingyu Sun[1], Toshihiro Ogawa[1], Hidenori Ojima[1], Kazuyoshi Takayama[1], and Joseph Falcovitz[3]

[1] Shock Wave Research Center,Institute of Fluid Science, Tohoku University, Sendai 980, Japan
[2] Department of Modern Mechanics, University of Science and Technology of China, Hefei, Anhui, 230026, China
[3] Institute of Mathematics, Hebrew University, Jerusalem 91904, Israel

Abstract. The interaction between a planar shock wave and a blast wave was investigated experimentally and numerically. Three types of interaction, namely a blast wave starts ahead, at, and behind a planar shock were considered. It was found that the flow configuration changes dramatically during different stages of the interaction. The comparison between the experiments and numerical simulation is helpful not only for better understanding of the phenomena, but also for improving the the numerical modeling of the explosive charge.

1 Introduction

A class of interesting shock wave phenomena, generated through the interaction of a planar shock wave and a spherical blast wave, is considered both experimentally and numerically. When a blast wave or explosion starts ahead of the shock wave, the interaction is that of a moving shock wave sweeping over a blast wave, during which various wave configurations can be observed because the process covers the entire range of intersection angles between the two wave fronts. Another type of interaction is the case where the explosion of the blast starts behind the planar shock wave, in which case only a part of the blast wave front can catch up with the planar shock. The intermediate case is a point source explosion that starts exactly at the planar shock front. Such an interaction has several typical characteristics: there is no length scale since the initial distance between the source of the explosion and the planar shock front is zero, and the two shocks interact from time zero on, with the strength of the blast wave decreasing while the incident shock is constant. The wave structure changes in time even though there is no length scale, since the blast wave is dominant at the initial stage and gets progressively overpowered by the planar shock at later times.

Based on the above considerations, we proceeded with the numerical and experimental study, aimed not only at obtaining an understanding of the phenomena, but also at improving numerical modeling of blast formation.

2 Experimental and Numerical Methods

The experiment was conducted in a highly repeatable diaphragmless shock tube, which has 60 mm×150 mm cross-sectional driven section [1]. To offer sufficient observation time for the blast wave, a large size test section with 150 mm×360 mm cross-section and 4 m long was connected to the downstream of the diaphragmless shock tube, and a specially designed smooth transition part was inserted in between to decrease the diffraction effect when the planar shock wave propagates through the divergent part. A 10 mg pellet of silver azide was mounted at the center of the test section, and was ignited by a YAG laser (Laser Photonics LTD, LPI Model/MYL-100), triggered by a pressure transducer located at a position 710 mm ahead of the pellet. An adjustable time-delay enabled any desirable timing of the charge initiation relative to the shock arrival. Double exposure holographic interferometry was used to visualize the flow.

In numerical simulation, propagation and interaction of shock waves were modeled by the axisymmetric Euler equations assuming an inviscid fluid with a perfect gas equation-of-state. The equations were solved numerically using a second-order TVD-type scheme on unstructured quadrilateral grids [2]. A solution-adaptive technique was employed to enhance the resolution of shock wave and contact regions. In general, grid cells were refined in regions having large density gradients, and coarsened in smooth regions. A six-level refinement was used in the present computations, and the minimum cell size was 1/64 cm. The initial conditions for the explosion products were a compressed quiescent gas sphere having the same energy and similar size as those of the charge.

3 Results and Discussions

As mentioned before, there are three types of interaction according to the position relationship. Figure 1 shows experimental interferograms of the two types, namely an explosion starts ahead of a moving planar shock wave (Fig. 1a) and an explosion is initiated at the instant when the moving planar shock meets the explosive (Fig. 1b). Figure 2 and Fig. 3 are the numerical results corresponding to the experimental conditions shown in Fig. 1a and Fig.1b, respectively. Figure 2a and Fig. 3a are integrated density contours for the direct comparison with the experiments, and Fig. 2b and Fig. 3b are isopycnics on cut-through plane for the detailed flow configuration. For the case of Fig. 1a and Fig. 2, the explosion started 50 micro-second before the planar shock arrives and the photo was taken 80 micro-second after the shock past the center of the explosion. The agreement between the experiment and the CFD results is good, although the center part of the interferogram looks a little disordered and the blast wave front somehow non-spherical because of non-spherical pellet and some scatter of the explosive. It is obvious that the planar shock front is strongly deformed when it enters the field covered by the blast wave: the center part going faster; the transmitted shock after the intersecting with the blast wave front became precursor and two kinks can be observed at the instant when the photo was taken.

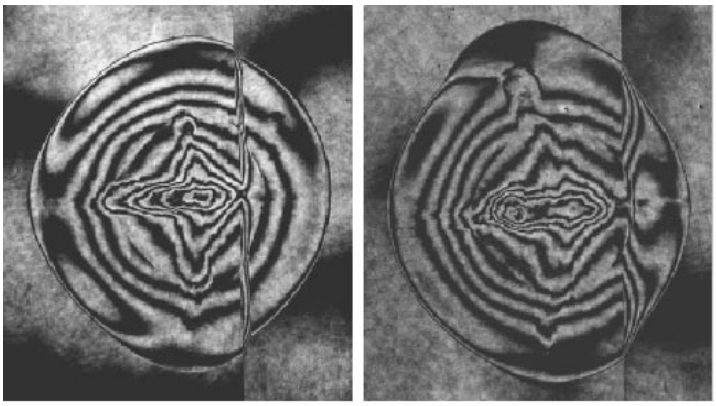

Fig. 1. Experimental interferogram. Ms=1.25. a, Planar shock interacts with blast wave initiated 20 mm ahead. Exposure time: 80μs after the shock past the center of explosion; b, Planar shock interacts with blast wave initiated at the shock front. Exposure time: 130μs after explosion

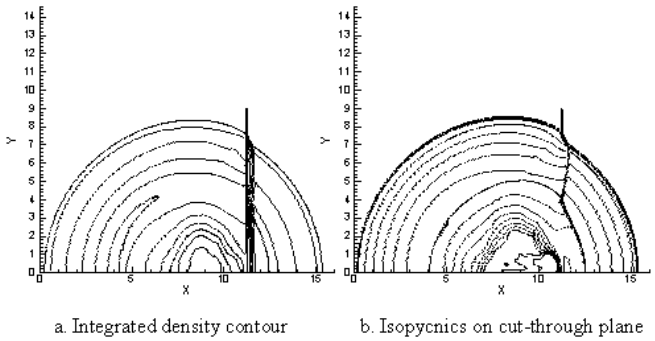

Fig. 2. Numerical simulation of a Planar shock interacts with blast wave initiated 20 mm ahead. 80μs after the shock past the center of explosion. Ms=1.25

For the case of Fig.1b and Fig. 3, the explosion started at the planar shock front, and the exposure time of the photo was 130 micro-second after the planar shock wave past the center of explosion. It can be found that the two wave fronts merged together after the intersection. The bulged part ahead of the planar shock is strongly curved like an S-shape, which demonstrates strength variation along this part and the strongest location is at the intersection point where the two shock merge. As it is well known that the concave part of this curved wave front is not stable and will undergo a self-focusing process and form a sharp discontinuity on the wave front at later time. It needs to be pointed

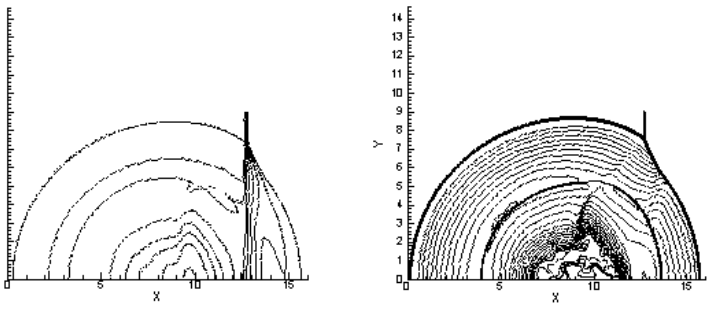

Fig. 3. Numerical Simulation of a Planar shock interacts with blast wave initiated at the shock front. 130μs after explosion

out that in the numerical simulation, the mass of the explosive should be taken into account to get good agreement with the experiment, which is more sensitive for the case of Fig. 3 than that of Fig. 2. Since the mass is added to the fluid after explosion, the flow field of the blast becomes quite different from that of point-source explosion, which suggests that the self-similar solution [3] is not adequate for the numerical initial condition in the cases considered here.

Following validation by the experiment, it is instructive to investigate the time development of the interaction through additional numerical simulation. In present experiment, it was difficult to generate strong planar shock wave because of the large divergent connection in the driven section of the shock tube and the shock Mach number in the above part was 1.25. Numerically we are free to choose parameters and it was found that more dramatic interaction might be in the case of strong shock wave. Fig. 4 shows numerically various stages of a planar shock of Mach number 2.0 sweeping over a blast wave which was ignited 1cm ahead. At the initial stage as shown in Fig. 4a, the planar shock wave intersects with the blast wave regularly, and the discontinuity of the wave fronts is at the intersection point. The transmitted shock front is bent backwards by high speed outward flow behind the blast wave. A part of the transmitted shock catches up and merges with the inward secondary shock. The configuration varies when it develops a little further as can be seen in Fig. 4b, the part of the blast wave front which is compressed by the planar shock jumps up compared to the uncompressed one and two kinks (or intersection points) are observable. The length of the segment connecting the two kinks increases with time and makes the bulged wave front approach a planar shape (Fig. 4c). On the other hand, the part of the transmitted shock which merged with the secondary shock approaches the center (Fig. 4b), and then together with the outward rebounded secondary shock, propagates with much higher speed and tends to overtake the outer blast wave front (Fig. 4c). It should be mentioned that the other strong density gradient which is observable behind the transmitted shock is a contact

region which was generated by the explosion and can be hardly observed from the pressure information. The hot central part of the explosion, having been swept by the planar shock, is strongly deformed and a rolling up of a vortex can be readily be observed with the help of numerical animation.

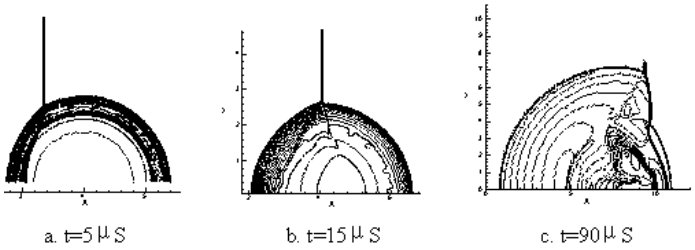

Fig. 4. Sequential numerical isopycnics of planar shock interacts with blast wave initiated 10mm ahead. Shock Mach number: 2.0, t=0 is the instant when the explosion starts.

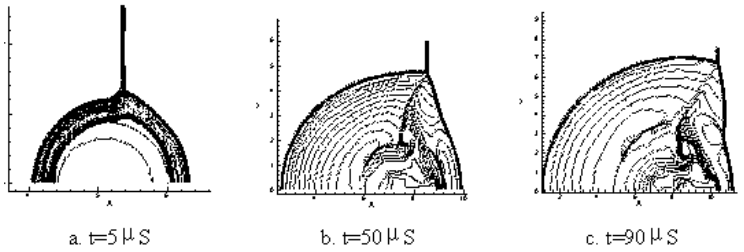

Fig. 5. Sequential numerical isopycnics of planar shock interacts with blast wave initiated at shock front. Shock Mach number: 2.0, t=0 is the instant when the explosion starts.

Fig.5 shows the time sequence of the interaction for the case where the explosion starts at the shock front, with shock Mach number 2.0. The shape of the wave structure is dominated by the blast wave at the early stage as shown in Fig. 5a, although it is not a circular shape, and a kink is formed on the blast wave front behind the planar shock, since the planar shock is fairly strong. As the blast wave decays, the bulged part ahead of the planar shock assumes an S-shape (Fig. 5b), and the concave part intensifies, forming another kink. Thus, it is possible to observe two kinks, one on each side of the main intersection point. Similarities can found between Fig. 5c and Fig. 4c, which suggests that both wave patterns approach the same configuration at large times.

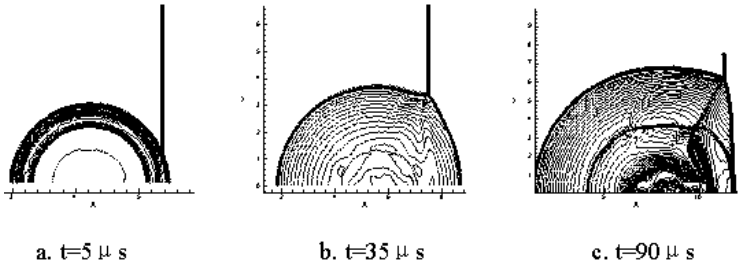

Fig. 6. Sequential numerical isopycnics of planar shock interacts with blast wave initiated 10mm behind. Shock Mach number: 2.0, t=0 is the instant when the explosion starts.

When the explosion starts behind the planar shock wave, the situation seems less complicated compared to the other two cases. The central part of the explosion seems less perturbed. But when the initial distance is short, a remarkable interaction will also occur between the strong blast wave and planar shock even though the blast comes from behind. As shown in Fig. 6, although it looks like a simple overtaking at the initial stage (Fig. 6a), a kink is formed on the compressed blast front when the strengths of the two shocks are comparable (Fig. 6b). The strong shear and non-isentropic layer induced by the intersection point causes a rolling-up process at the later stage of the interaction (Fig. 6c), which is similar to the case shown in Fig. 5c.

As a final remark, it needs to be mentioned that there is still a considerable potential for improvement of initial condition in the numerical simulation, since the explosive used in the experiment is simply modeled by energy and mass input approximation, neither detonation process in the explosive nor changes in gas properties were taken into account. Consequently, a more careful modeling of the explosive charge is called for.

References

1. Yang J, Onodera O, Takayama K (1994) Experimental study of weak shock wave generation. Proc. 3rd JSME-KSME Fluid Engineering Conference. PP. 606-609
2. Sun M, Takayama K (1999) Conservative smoothing on an adaptive quadrilateral grid. J Comp Phys **150**, PP. 143-180.
3. Jiang Z, Takayama K, Moosad KPB et al (1998) Numerical and experimental study of a micro-blast wave generated by pulsed-laser beam focusing. J Shock Waves. **8**, PP.337-349.
4. Higashino F, Henderson LF, Shimizu F (1992) Experiments on the interaction of a pair of cylindrical weak blast waves in air. J Shock Waves, **1**, PP.275-284